

# Corrosivity of environment and the current state of the steel elements at the former Auschwitz concentration camp

**Andrzej Miszczyk, Michal Szocinski, Kazimierz Darowicki**

Chemical Faculty, Department of Electrochemistry, Corrosion and Materials Engineering, Gdansk University of Technology, Gdansk, Poland

The objective of this study was to assess corrosivity of the atmospheric environment in the former Auschwitz I and Auschwitz II-Birkenau concentration and extermination camp, and to identify the protective properties of existing corrosion products in order to estimate the actual corrosion rate of original steel elements located there. The current atmospheric corrosivity of the former Auschwitz camp, specified during one year of exposure of steel samples according to the EN ISO 12944-2 (1998) standard, was determined and it can be described as a boundary between the low C2 and medium C3. The steel corrosion rate in these conditions was in the range of 14–34  $\mu\text{m}/\text{year}$  with the average rate of 27  $\mu\text{m}/\text{year}$ . A layer of corrosion products formed on uncovered original reinforcement steel rods during ca. 70 years of atmospheric exposure was examined in terms of their protective properties with respect to steel. The microstructure, chemical composition, and elemental chemical state were analyzed by means of scanning electron microscopy equipped with energy-dispersive X-ray spectroscopy, X-ray photoelectron spectroscopy, and X-ray diffraction. Potentiodynamic polarization and electrochemical impedance spectroscopy methods were employed to investigate the corrosion resistance of the carbon steel covered with a layer of corrosion products. It has been estimated that this layer slows down the corrosion rate of steel by about five times. Hence, it can be concluded that the corrosion rate of the original steel parts under the layer of corrosion products should not exceed 7  $\mu\text{m}/\text{year}$ .

**Keywords:** Cultural heritage, Corrosion, Environmental factors, Corrosivity, Degradation, Preservation

## Introduction

KL Auschwitz was the largest of the German Nazi concentration and extermination camps during World War II. Over 1.1 million people lost their lives there. This area is now the Auschwitz-Birkenau State Museum, which is visited annually by over 1.5 million people from all over the world ([Auschwitz Report, 2014](#)). The museum consists of two distinct areas: Auschwitz I (the older part, founded in 1940) and Auschwitz II-Birkenau (founded in 1942), located at a distance of about 3 km from each other and situated in or near the town Oswiecim. The whole area of the former camp Auschwitz is ca. 200 ha. The museum is obliged to care and preserve buildings, watchtowers, ruined gas chambers and

crematoria, water treatment plants, shelters, as well as railroad tracks, roads, irrigation/drainage ditches, sewers, fences, and gates in this area.

After more than 70 years of exposure, the former concentration and extermination camps Auschwitz I and Auschwitz II-Birkenau need assessment of the current state of buildings, ruins, and other architectural elements to undertake necessary comprehensive maintenance. It is obvious that this memorial to the tragic events of World War II, and a symbol of the Holocaust and Nazi German crimes, is a warning to the world never to forget this tragic historical event and it should be preserved as intact as possible for future generations. Many former Nazi concentration and extermination camps have not been maintained in their original form — they have been partially dismantled, leaving only fragments as memorials or they have disappeared completely. No doubt there are voices calling for the efforts towards preservation of Auschwitz as probably the last such piece of cultural

heritage witnessing the Holocaust and Nazi atrocities (Weissberg, 1999; Charlesworth & Addis, 2002; Taylor, 2015).

All camp components have been exposed to atmospheric conditions and subjected to varying humidity and temperature, as well as to chemical contamination. The geographical location of the former concentration camp, near two large rivers (Vistula and Sola) resulted in high groundwater levels and hence high atmospheric humidity. In these conditions, the risk of biodegradation and microbiological corrosion must be taken into account and these have previously been identified onsite (Nowicka-Krawczyk *et al.*, 2014; Rajkowska *et al.*, 2014).

In order to preserve these historic structures effectively, it is necessary to identify and characterize the local environmental conditions, identify the materials used in manufacturing the components on the site, and assess the rate of their deterioration (Crevello *et al.*, 2015; Pascoal *et al.*, 2015). This is of particular importance since there has been clear preference for minimum intervention during conservation in order to maintain authenticity of the former camp (Scott, 2015). Corrosivity of the total environment is a sum of contributions from atmospheric effect along with local water and soil chemistries that have the potential to negatively impact the condition of the structures. Therefore, the assessment of the *in situ* corrosion is not an easy task. The most general approach to this evaluation is the determination of the corrosion rate of the most frequently used construction material, which was identified as a low carbon steel (Natesan & Palaniswamy, 2009; De la Fuente *et al.*, 2011), following the European Standard EN ISO 12944-2 (1998).

A comprehensive evaluation of present environmental effects on corrosion of the museum area and the state of selected steel elements from the former Auschwitz camp are presented here. Similar procedures have been used in many situations to assess the risks of destruction of architectural buildings and structures over long durations in air (Rincon *et al.*, 2000; Chico *et al.*, 2010; Vera *et al.*, 2011; Agbota *et al.*, 2013; De la Fuente *et al.*, 2013; Karaca, 2013; Kumar & Imam, 2013; Surnam, 2015) or in soil (Ferreira *et al.*, 2007; Kibblewhite *et al.*, 2015). This study will allow for the selection of adequate conservation and protection methods in addition to providing insight into localized climate changes, if such a study will be repeated in the future (Kumar & Imam, 2013).

This study is part of a larger effort to develop a comprehensive conservation and protection programme for the former camp. The next step will be an assessment of concrete structures and the influence of the local environment on their condition (paper in preparation).

**Table 1 Atmospheric corrosion categories according to EN ISO 12944-2 (1998)**

Corrosion category	Mild steel corrosion rate (1 year of exposure) ( $\mu\text{m}/\text{year}$ )
C1	$\leq 1.3$
C2	1.3–25
C3	25–50
C4	50–80
C5-I	80–200
C5-M	80–200

## Materials and methods

The corrosivity of the atmosphere at the former Auschwitz camp was examined by measuring the rate of corrosion loss of carbon steel plates in accordance with the EN ISO 12944-2 (1998) standard (European standard, EN ISO 12944-2 Paints and varnishes — Corrosion protection of steel structures by protective paint systems — Part 2: Classification of environments). This standard specifies the corrosion categories from C1 to C5. They depend on the corrosion loss on steel as shown in Table 1.

Table 2 provides some examples of related corrosion environments. It was decided to assess the corrosivity of the environment following these categories.

Steel corrosion rates were determined in different locations (Table 3) around Auschwitz I and Auschwitz II-Birkenau, based on a gravimetric method (i.e. on the basis of the sample mass loss due to corrosion in a given period of time).

Samples of carbon steel (dimensions of 4 cm  $\times$  5 cm  $\times$  1 mm) were deployed in duplicate (to ensure reproducibility of results) at different locations of the camp (Fig. 1) for the period of one year (from 02.06.2014 to 02.06.2015). They were sanded using sandpaper with gradation up to P240 (grit sizes

**Table 2 Examples of typical atmospheric corrosion environments**

Corrosion category	Examples of typical corrosion environments
C1 very low	Heated buildings with clean atmospheres inside, e.g. offices, shops, hotels
C2 low	Atmospheres with low level of pollution, mostly rural areas; Buildings unheated inside, where condensation may occur
C3 medium	Urban and industrial atmospheres, moderate sulphur dioxide pollution, coastal areas with low salinity
C4 high	Industrial areas and coastal areas with moderate salinity
C5-I very high, industrial	Areas or buildings with almost permanent condensation with high level of pollution, chemical plants
C5-M very high, marine	Coastal and offshore areas with high salinity

**Table 3** The exposure sites of the steel samples for determination of environment corrosivity in the former Auschwitz concentration and extermination camp

Sample number	Part of the camp	Exposure site
1	Auschwitz I	A park outside the building of Auschwitz camp commandant
2	Auschwitz I	Façade of the crematorium no. 1
3	Auschwitz I	A fence at the block no. 24 (next to the main entrance)
4	Auschwitz I	A fence at the building 'G' (now the seat of the Conservation Department)
5	Auschwitz I	A fence at the block no. 18
6	Auschwitz I	A fence at the block no. 11
7	Auschwitz I	A fence at the block no. 5
8	Auschwitz II-Birkenau	Ruined fence at the border of so called Mexico part of the camp
9	Auschwitz II-Birkenau	Vicinity of the sprinklers
10	Auschwitz II-Birkenau	An electric post near the ruins of crematorium no. 3
11	Auschwitz II-Birkenau	Inside the ruins of crematorium no. 2
12	Auschwitz II-Birkenau	A fence in vicinity of the ruins of crematorium no. 2
13	Auschwitz II-Birkenau	Front façade of the pumping station
14	Auschwitz II-Birkenau	A fence in vicinity of the pumping station
15	Auschwitz II-Birkenau	A door frame of the sprinkler
16	Auschwitz II-Birkenau	Front façade of one of the watchtowers
17	Auschwitz II-Birkenau	Ruined fence at the border of so called Mexico part of the camp (next to present road)
18	Auschwitz II-Birkenau	Next to the water reservoir, section BIIc
19	Auschwitz II-Birkenau	A fence at the right side of main entrance A
20	Auschwitz II-Birkenau	Place next to the foundations of the hospital barracks
21	Auschwitz II-Birkenau	A fence next to railroad platform

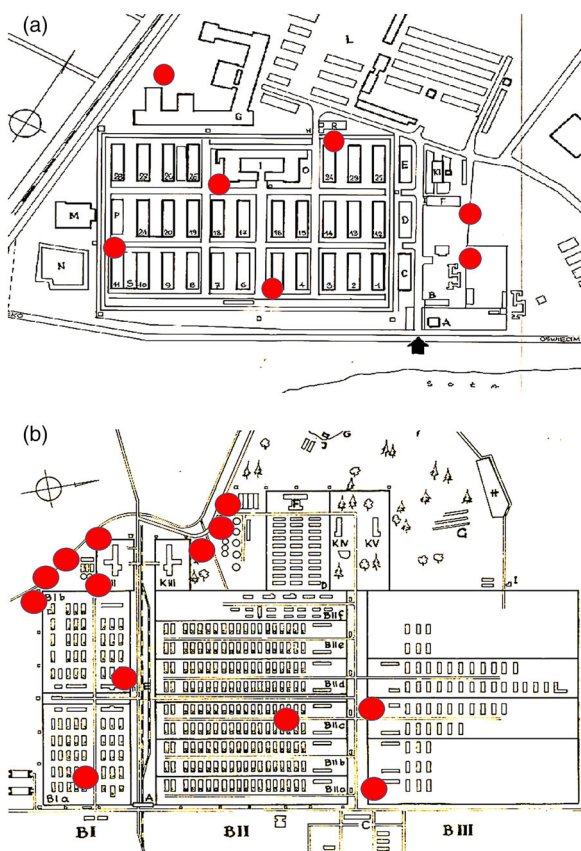


**Figure 1** Places of exposure of steel samples for corrosivity tests in Auschwitz I (A) and Auschwitz II-Birkenau (B).

according to ISO 6344-3 standard) to obtain a clean metal surface, washed in distilled water, degreased with acetone and weighed. Slightly smaller samples were used in locations requiring more discretion, either based on the sensitivity of the testing location, or due to potential damage or loss arising from the presence of more than 1.5 million visitors during the time of exposure. The locations chosen for sample exposure were meant to correspond with the locations of original steel elements from the former Auschwitz camp infrastructure. Samples numbered 1–7 were placed in Auschwitz I, and samples numbered 8–21 were placed in Auschwitz II-Birkenau. Fig. 2 shows the appearance of the samples after one year of exposure. Fig. 3 shows the climatic parameters of camp location during one year. After one year, the samples were retrieved, rinsed with water, and immersed in a 10% solution of hydrochloric acid containing a steel corrosion inhibitor. The samples were then thoroughly washed with distilled water, dried and weighed to an accuracy of 0.1 mg.

The corrosion rate  $v$  was determined according to the formula:

$$v = \frac{m_1 - m_0}{St} \quad (1)$$

where  $m_1$  is the sample mass before exposure,  $m_0$  is the sample mass after exposure, without corrosion products,  $S$  is the surface of the sample,  $t$  is the time of exposure.

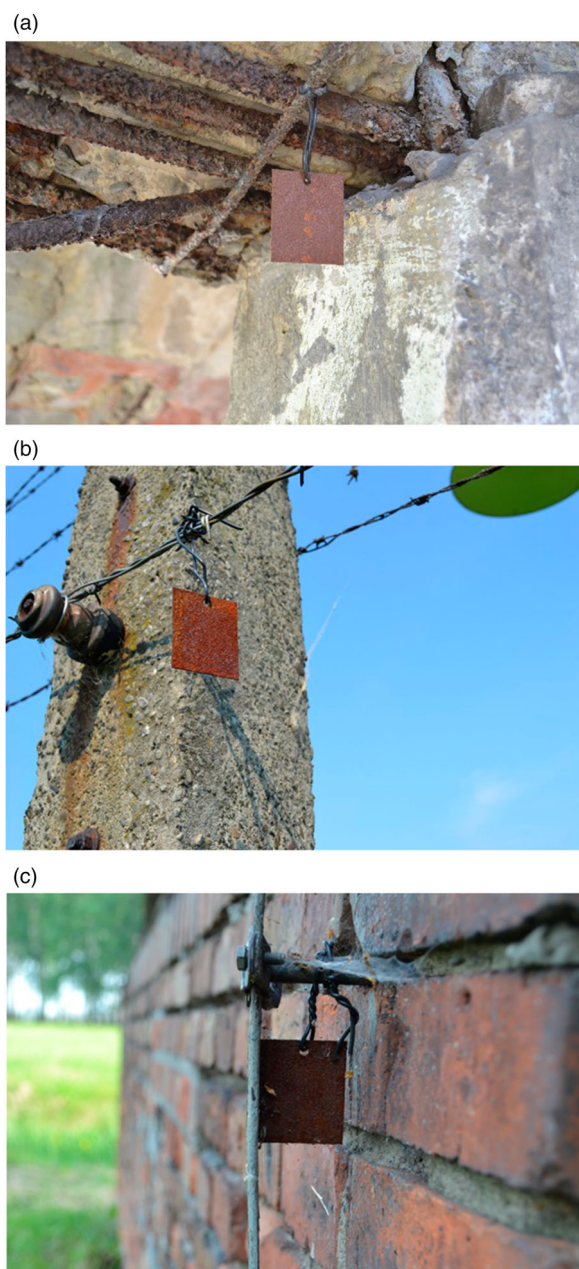


**Figure 2** Sample No. 6 exposed in the ruins of the crematorium II in Auschwitz II-Birkenau (A), sample No. 9 exposed on the fence of Auschwitz II-Birkenau (B), sample No. 11 exposed at the brick front of the watchtower in Auschwitz II-Birkenau (C) after one year of exposure.

The accuracy of corrosion rate determination was made using the method of total differential:

$$\Delta v(m, S, t) = \left| \left( \frac{\partial v}{\partial m} \right) \right| \Delta m + \left| \left( \frac{\partial v}{\partial S} \right) \right| \Delta S + \left| \left( \frac{\partial v}{\partial t} \right) \right| \Delta t \quad (2)$$

where  $(\partial v / \partial m)$ ,  $(\partial v / \partial S)$ , and  $(\partial v / \partial t)$  partial differential with respect to the variable  $m$ ,  $S$ , and  $t$ , respectively, at the measurement point,  $\Delta m$  is the measurement error of mass determination,  $\Delta S$  is the measurement error of surface determination, and  $\Delta t$  is the measurement error of exposure time determination.

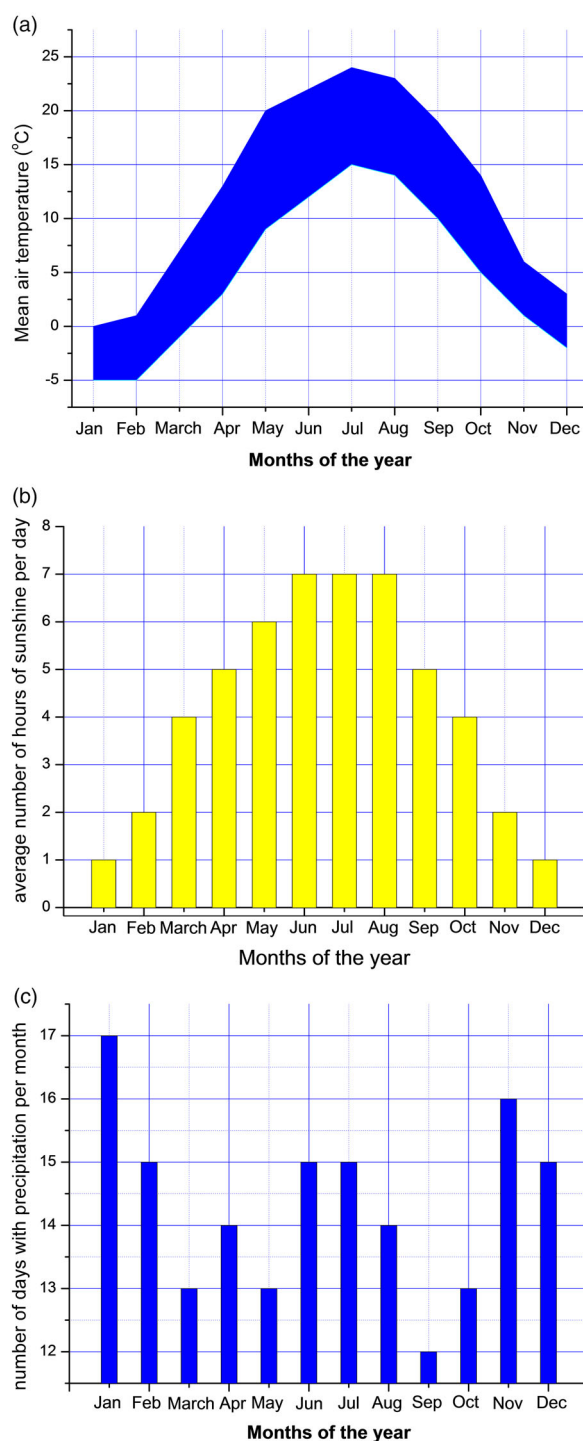


**Figure 3** Characteristics of the climate of the town Oswiecim, where the former Auschwitz concentration and extermination camp is situated. Graphs based on data obtained from local meteorological station for the last 10 years.

The maximum measurement error estimated in this way did not exceed 7%. The results of visual inspection revealed that in all cases the entire sample surface was covered with a relatively uniform layer of corrosion products.

X-ray diffraction patterns (XRD) were recorded using an X'Pert Pro diffractometer with CuK $\alpha$  radiation. The scans were collected in the  $2\theta$  range of

20–124°. Phase identification was performed with X'Pert High Score Plus software using the JCPDS database.

Scanning electron microscope (SEM) analysis was performed using a Hitachi S-3400N microscope. Secondary electron micrographs were taken at 20 kV accelerating voltage. The microscope was equipped with a ThermoFisher Scientific EDX detector.

The analysis was supplemented using the X-ray photoelectron spectroscopy (XPS) technique. A ThermoFisher Scientific XPS Escalab 250Xi spectroscope was used. The diameter of the spot of the radiation source was 200  $\mu\text{m}$ . Depth profiling using an ion gun (500 V) was performed.

## Results and discussion

The average corrosion rates of mild steel samples after one year of exposure were determined. Fig. 4 presents the results for each location. Sample No. 6's lower corrosion rate is most likely due to the fact that it was sheltered from the top (the ruins of the crematorium II in Auschwitz II-Birkenau, Fig. 5). Sample No. 10 was also sheltered (in the sprinkler in Auschwitz II-Birkenau). The data shows that currently the corrosive atmosphere of the former Auschwitz camp can be placed between a low C2 and a medium C3 corrosivity (Table 1). The impact on the corrosivity partially originates from the presence of the town Oswiecim and the local industrial chemical plant but this influence is not considered significant, which is indicated by obtained corrosion rates (Fig. 4) characteristic for rural atmospheres.

Moreover, the investigation included the examination of exposed steel reinforcement elements after approximately 70 years of exposure in the ruins of the crematorium. At the end of the war the retreating

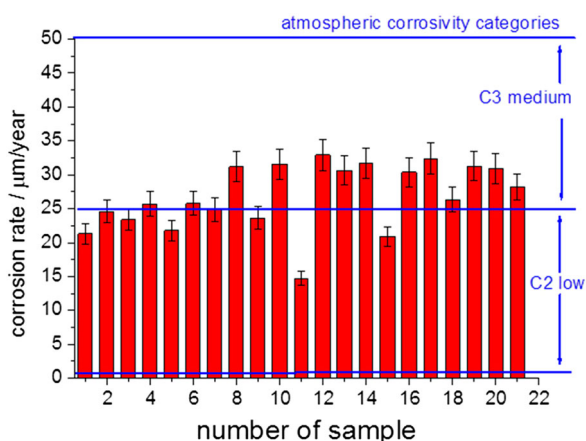


**Figure 4** The corrosion rate of carbon steel in different places at Auschwitz I (1–7) and Auschwitz II-Birkenau (8–21). Maximum measurement error determined by the total differential is marked. Ranges of small and medium corrosivity categories in accordance with EN ISO 12944-2 (1998) indicated.

Germans blew up the crematoria. As a result some of the reinforcing bars were uncovered in the ruins (Fig. 5) and have been exposed to the ambient environment until now. Metallographic analysis (Gotkowski & Jachym, 2014) of 42 different original steel samples showed that the steel used is ferrite-perlite type, similar to the composition of the present steel S235JR (Europe) or A283 Gr. C (USA). Full representative exemplary analysis is shown in Table 4.

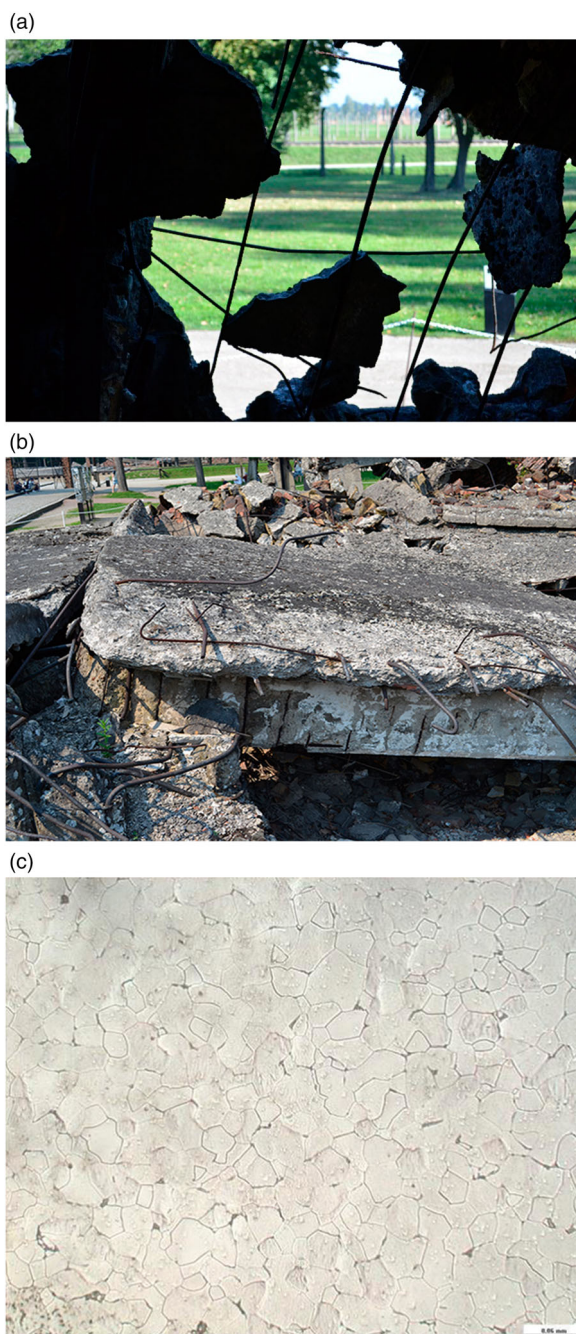


**Figure 5** Uncovered reinforcing steel bars of the ruins of the crematorium II in Auschwitz II-Birkenau (A), a ceiling of the gas chamber of this crematorium (B), and the metallographic structure (grainy ferrite and very small amounts of perlite, several non-metallic inclusions, magnification 200 $\times$ ) of the reinforcing bar adopted from Gotkowski & Jachym, 2014 (C).

**Table 4 Exemplary chemical composition of steel from the Auschwitz-Birkenau State Museum determined using an emission spectrometer with spark excitation (Gotkowski & Jachym, 2014)**

Element	C	Si	Mn	P	S	Cr	Mo	Ni	Cu	Al	As
Content %	0.139	0.002	0.418	0.038	0.035	0.007	0.003	0.02	0.224	<0.001	0.038
Element	Bi	Ce	Co	Nb	Pb	Sb	Sn	Ti	V	W	Zr
Content %	0.01	0.003	0.009	0.003	<0.003	0.028	0.009	<0.001	<0.001	0.005	<0.001

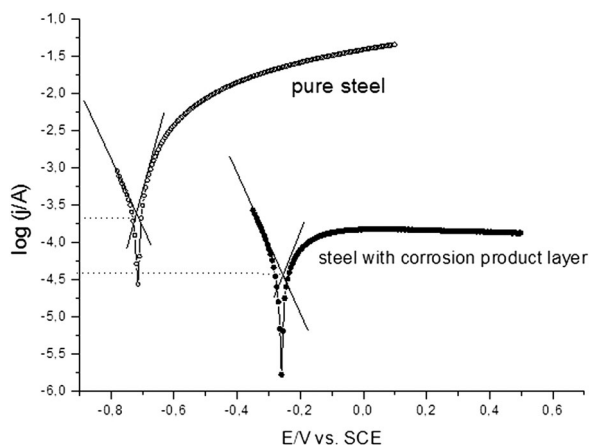


**Figure 6 Potentiodynamic curves obtained for the samples of rebar (original diameter of 10 mm) with corrosion products and after their removal (bare steel). SCE, saturated calomel electrode.**

Electrochemical tests were performed using several original rods in two states: covered with corrosion products and without corrosion products (after etching in 10% HCl solution with corrosion inhibitor). The results of the tests presented below are exemplary ones as all the samples behaved in very similar way. Fig. 6 shows the typical polarization curves obtained in both cases. The determined values of corrosion current densities, directly accountable for the rate of corrosion (based on the first Faraday's law) are shown in Table 5. The data obtained reveal that the existing layer of corrosion products possesses a protective function, lowering by approximately five times the steel corrosion rate. This is confirmed by the results of impedance measurements (Figs. 7 and 8). Impedance spectroscopy is widely used to examine the protective properties of the coating ( e.g. Miszczyk *et al.*, 2007; Lvovich, 2012; Miszczyk & Darowicki, 2014) and

**Table 5 Corrosion current densities ( $i_{corr}$ ) and corrosion rate ( $v_{corr}$ ) of the steel samples**

Sample	$i_{corr}/Acm^2$	$v_{corr}/\mu m/year$
1 A steel rod with a layer of corrosion products	$3.7 \times 10^{-5}$	28.8
2 A steel rod without corrosion products	$2.0 \times 10^{-4}$	155.7

other layers on metal. Obtained spectra are modelled using appropriate electrical equivalent circuits. Each element of the equivalent circuit has a physical meaning, which also takes into account the relation to barrier properties. In this way it is also possible to quantitatively evaluate the barrier properties of a rust layer (Singh *et al.*, 2008). Obtained impedance values are about five times greater in the case of the sample with corrosion products. Hence, it can be concluded that the corrosion rate of the original steel parts under the layer of corrosion products should not exceed  $7 \mu m/year$ .

In order to examine the composition of the corrosion products of steel, a cross section of the rod was made (Fig. 9) and SEM measurements were performed. The result of energy-dispersive X-ray spectroscopy (EDX) measurements in an exemplary point is presented in Fig. 10. The composition of the rust layer includes calcium, as a remnant of the

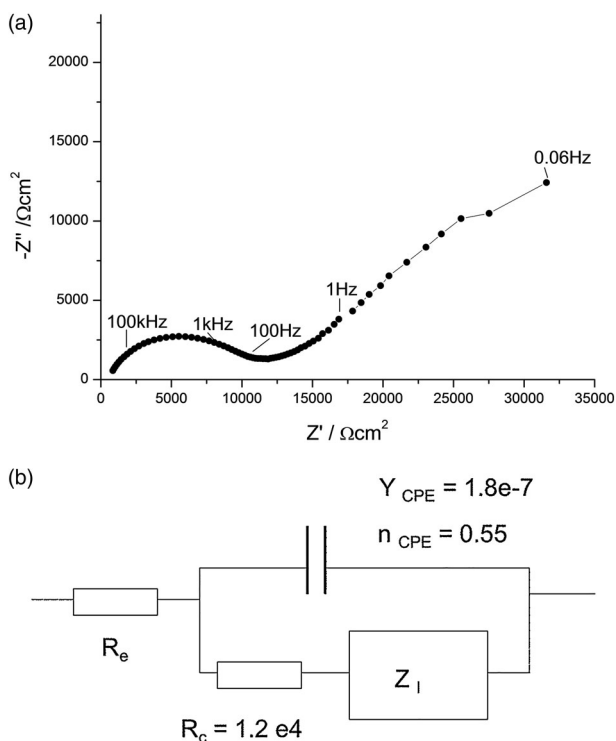


**Figure 7 The impedance spectrum in a Nyquist format of the mild steel rebar with a layer of rust exposed in the ambient atmosphere of Auschwitz II-Birkenau during ca. 70 years (A) and corresponding electrical equivalent circuit (B).**

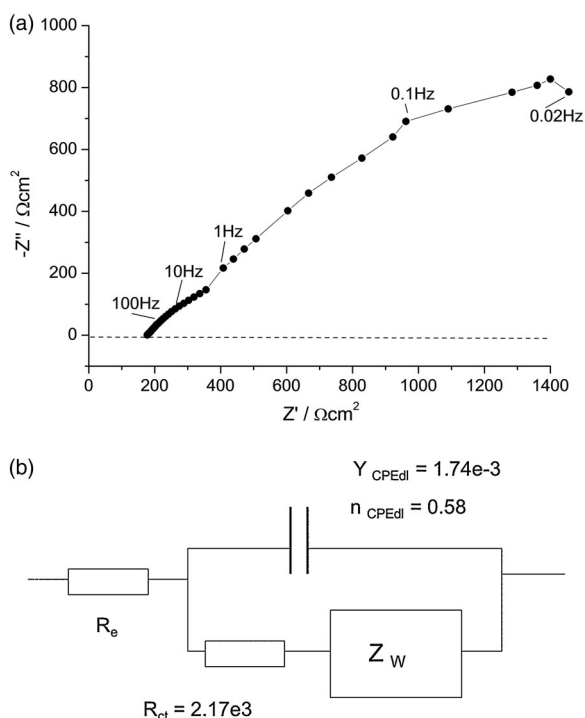


**Figure 8** The impedance spectrum in a Nyquist format of the mild steel rebar without layer of rust (A) and corresponding electrical equivalent circuit (B).

concrete cover of the rod. The beneficial effect of calcium ions on the protective properties of the rust layer was observed (Karman *et al.*, 1998). Additional studies using XPS show that calcium is in the form of carbonate and oxide (Fig. 11). Most probably they strengthen the protective properties of the layer of corrosion products. The composition of corrosion products collected in Auschwitz I and Auschwitz II-Birkenau was also examined with XRD (Fig. 12), which detected mainly magnetite  $Fe_2O_3$  and lepidocrocite  $\gamma-FeOOH$  and partially amorphous components. Such a composition of the corrosion products suggests a picture of typical steel corrosion under conditions of high moisture and high oxygen availability (no industrial pollutants usually rich in sulphur are present and there is a little contribution of sulphur in the rust layer as illustrated in Fig. 10) (Hiller, 1966). Results show that this layer reveals relatively good adhesion to the steel substrate and contains a stable form of iron oxides saturated with calcium carbonate originating from the concrete cover. There are several types of carbon steel corrosion products (Hiller, 1966) with different ratios: volume of corrosion products to volume of the corresponding iron from which the oxide is created (the Pilling-Bedworth ratio). The products with a high ratio ( $>2$ , non-protective) were naturally flaked off during 70 years of atmospheric exposure. The products with a low ratio ( $<2$ , protective, according to the Pilling-Bedworth rule) remained on the surface creating an

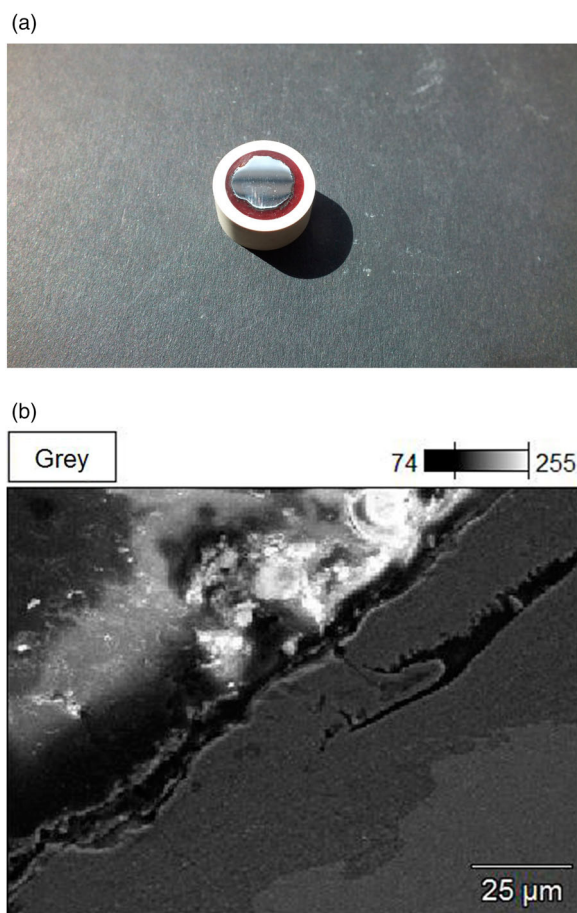


**Figure 9** Cross-sectional photo (A) and SEM image (B) of a bare rebar rod with corrosion products exposed to ambient atmosphere of Auschwitz II-Birkenau without cover. The micrograph shows a sectional layer of corrosion products.

adherent and relatively protective layer. A similar situation occurs for steel rebars embedded in concrete where protective iron oxide (with low Pilling–

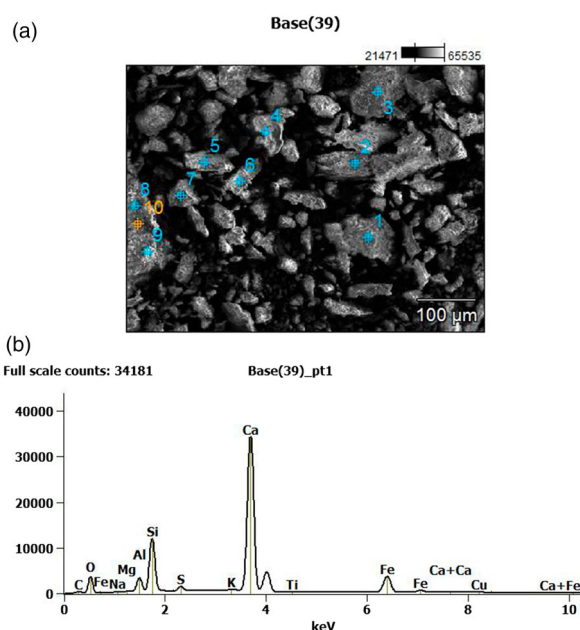


**Figure 10** Layer of corrosion products on steel rod (A) and exemplary EDX result for point 1 (B).

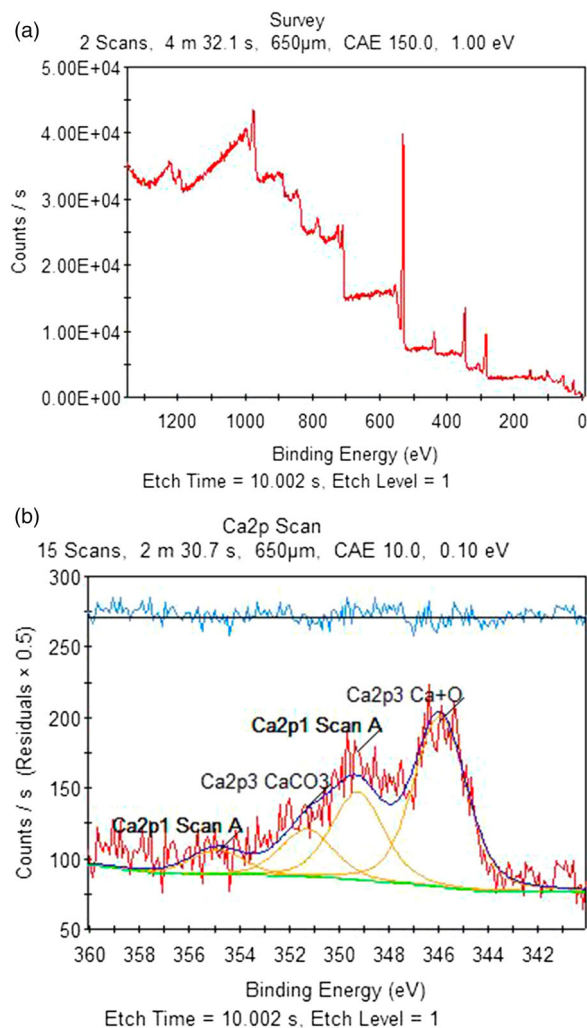


**Figure 11** Results of XPS measurements of steel corrosion products.

Bedworth ratio) forms a passive layer. This effect is strengthened by the presence of calcium carbonate (like it is in the case of rocks) and calcium oxide (like in concrete). The presence of calcium carbonate and calcium oxide was confirmed in XPS tests.

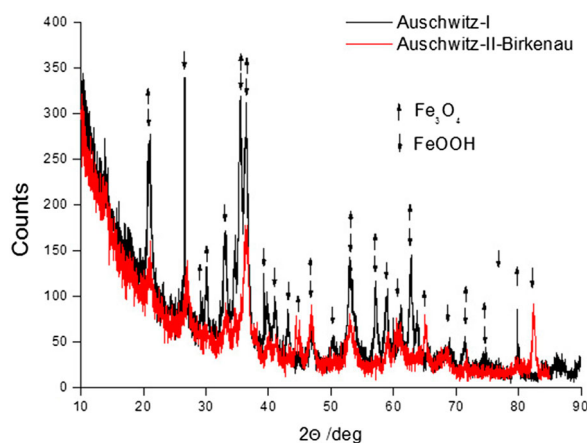


**Figure 12** XRD spectrum of rust collected from exposed uncovered reinforcement steel rod.

Electrochemical investigations made it possible to determine the actual corrosion rate of steel structures of the former Auschwitz camp, and thus, a prediction of their lifetime could be established with higher accuracy. Moreover, knowing the precise corrosion rate of steel in these conditions, one is able to select suitable protective measures. In this case, the treatment does not need to be invasive and uncompromising, which is of high importance for these historic structures.

## Conclusions

Based on the results obtained from the corrosion studies undertaken at the former Auschwitz concentration and extermination camp five main conclusions can be stated.

1. The current corrosivity of the atmosphere, specified during one year of exposure of steel samples according to the EN ISO 12944-2 (1998) standard, was determined to be located at the boundary between the low C2 and medium C3.
2. The steel corrosion rate in these conditions was in the range of 14–34  $\mu\text{m}/\text{year}$  with the average rate of 27  $\mu\text{m}/\text{year}$ .
3. The layer of corrosion products formed on uncovered reinforcement steel rods during ca. 70 years of atmospheric exposure was examined in terms of its protective properties. It has been estimated that this layer slows down the corrosion rate of steel by about five times. This finding allows for a more precise corrosion rate of steel structures of the former Auschwitz camp to be determined and allows us to predict their lifetime with higher accuracy and identify suitable potential protective measures.
4. Hence, it can be concluded that the corrosion rate of the original steel parts under the layer of corrosion products should not exceed 7  $\mu\text{m}/\text{year}$ .
5. The layer of corrosion products on the reinforcing steel rods consists mainly of magnetite ( $\text{Fe}_2\text{O}_3$ ) and lepidocrocite ( $\gamma\text{-FeOOH}$ ) with a small addition of calcium carbonate ( $\text{CaCO}_3$ ) and oxide ( $\text{CaO}$ ).

The study presented will be used to control the state of steel elements present in the former Auschwitz camp and to select possible methods for their conservation and protection. Determination of corrosivity of the atmosphere was an indispensable step as it established a starting point for corrosion risk assessment. When repeated periodically, it will allow monitoring and identification of any changes in aggressiveness of the environment with respect to the structures to be protected. Tracing the evolution of corrosivity of the atmosphere will make it possible to adjust the protective measures undertaken to maintain the structures of Auschwitz I and Auschwitz II-Birkenau in a preserved and least-interfered condition.



## Acknowledgments

The study was conducted as part of the Master Plan for Preservation at the Auschwitz-Birkenau State Museum.

## References

- Agbota, H., Young, C. & Strlic, M. 2013. Pollution Monitoring at Heritage Sites in Developing and Emerging Economies. *Studies in Conservation*, 58: 129–44.
- Auschwitz Report. 2014. News dated 05-08-2015 [accessed 10 August 2016]. Available at: <<http://auschwitz.org/en/museum/news/>>
- Charlesworth, A. & Addis, M. 2002. Memorialization and the Ecological Landscapes of Holocaust Sites: The Cases of Płaszow and Auschwitz-Birkenau. *Landscape Research*, 27: 229–51.
- Chico, B., De la Fuente, D., Vega, J.M. & Morcillo, M. 2010. Corrosivity Maps of Spain for Zinc in Rural Atmospheres. *Revista Metalurgia*, 46: 485–92.
- Crevello, G., Hudson, N. & Noyce, P. 2015. Corrosion Condition Evaluations of Historic Concrete Icons. *Case Studies in Construction Materials*, 2: 2–10.
- De la Fuente, D., Díaz, I., Simancas, J., Chico, B. & Morcillo, M. 2011. Long-term Atmospheric Corrosion of Mild Steel. *Corrosion Science*, 53: 604–17.
- De la Fuente, D., Vega, J.M., Viejo, F., Diaz, I. & Morcillo, M. 2013. Mapping Air Pollution Effects on Atmospheric Degradation of Cultural Heritage. *Journal of Cultural Heritage*, 14: 138–45.
- European standard, EN ISO 12944-2. 1998. Paints and Varnishes — Corrosion Protection of Steel Structures by Protective Paint Systems — Part 2: Classification of Environments. Brussels: European Committee for Standardization.
- Ferreira, C.A.M., Ponciano, J.A.C., Vaitsman, D.S. & Perez, D.V. 2007. Evaluation of the Corrosivity of the soil through its chemical composition. *Science of the Total Environment*, 388: 250–55.
- Gotkowski, P. & Jachym, R. 2014. Unpublished Report No. ZB/10/2014. Gliwice, Poland: Welding Institute (report available at the Auschwitz-Birkenau State Museum, Oswiecim, Poland).
- Hiller, J.-E. 1966. Phasenumwandlungen im Rost. *Werkstoffe und Korrosion*, 17: 943–95.
- Karaca, F. 2013. Mapping the Corrosion Impact of Air pollution on the Historical Peninsula of Istanbul. *Journal of Cultural Heritage*, 14: 129–37.
- Karman, F.H., Felhosi, I., Kalman, E., Cserny, I. & Kover, L. 1998. The Role of Oxide Layer Formation during Corrosion Inhibition of Mild Steel in Neutral Aqueous Media. *Electrochimica Acta*, 43: 69–75.
- Kibblewhite, M., Gergely, T. & Hermann, T. 2015. Predicting the Preservation of Cultural Artefacts and Buried Materials in Soil. *Science of the Total Environment*, 529: 249–63.
- Kumar, P. & Imam, B. 2013. Footprints of Air Pollution and Changing Environment on the Sustainability of Built Infrastructure. *Science of the Total Environment*, 444: 85–101.
- Lvovich, F. 2012. *Impedance Spectroscopy. Applications to Electrochemical and Dielectric Phenomena*. Hoboken, NJ: Wiley.
- Miszczyk, A. & Darowicki, K. 2014. Multivariate Analysis of Impedance Data Obtained for Coating Systems of Varying Thickness Applied on Steel. *Progress in Organic Coatings*, 77: 2000–06.
- Miszczyk, A., Szocinski, M. & Darowicki, K. 2007. Interlayer Defect Evolution in an Organic Coating System on Steel under Hydromechanical Loading. *Journal of Applied Electrochemistry*, 37: 353–58.
- Natesan, M. & Palaniswamy, N. 2009. Atmospheric Corrosivity and Durability Maps of India. *Corrosion Reviews*, 27 (Supplement): 61–112.
- Nowicka-Krawczyk, P., Zelazna-Wieczorek, J., Otlewska, A., Kozirog, A., Rajkowska, K., Piotrowska, M., Gutarowska, B. & Zydzik-Bialek, A. 2014. Diversity of an Aerial Phototrophic Coating of Historic Buildings in the Former Auschwitz II-Birkenau Concentration Camp. *Science of the Total Environment*, 493: 116–23.
- Pascoal, P., Borsoi, G., Veiga, R., Faria, P. & Silva, A.S. 2015. Consolidation and Chromatic Reintegration of Historical Renders with Lime-based Pozzolanic Products. *Studies in Conservation*, 60: 321–32.
- Rajkowska, K., Otlewska, A., Kozirog, A., Piotrowska, M., Nowicka-Krawczyk, P., Hachulka, M., Wolski, G.J., Kunicka-Styczynska, A., Gutarowska, B. & Zydzik-Bialek, A. 2014. Assessment of Biological Colonization of Historic Buildings in the Former Auschwitz II-Birkenau Concentration Camp. *Annals of Microbiology*, 64: 799–808.
- Rincon, A., De Rincon, A.I., Fernandez, M. & Loaiza, E. 2000. Measurement of Pollution Atmospheres in a Tropical Region and its Atmospheric Corrosivity Maps. *Corrosion Reviews*, 18: 473–87.
- Scott, D.A. 2015. Conservation and Authenticity: Interaction and Enquiries. *Studies in Conservation*, 60: 291–305.
- Singh, D.D.N., Yadav, S. & Saha, J.K. 2008. Role of Climatic Conditions on Corrosion Characteristics of Structural Steels. *Corrosion Science*, 50: 93–110.
- Surnam, B.Y.R. 2015. Three Years Outdoor Exposure of Low Carbon Steel in Mauritius. *Anti-Corrosion Methods and Materials*, 62: 246–52.
- Taylor, J. 2015. Embodiment Unbound: Moving Beyond Divisions in the Understanding and Practice of Heritage Conservation. *Studies in Conservation*, 60: 65–77.
- Vera, R., Puentes, M., Araya, R., Rojas, P. & Carvajal, A. 2011. Atmospheric Corrosion Map of Chile: Results after One Year of Exposure. *Revista Construction*, 11: 61–72.
- Weissberg, L. 1999. Memory Confined. In: D. Ben-Amos & L. Weissberg, eds. *Cultural Memory and the Construction of Identity*. Detroit: Wayne State University Press, pp. 45–76.